Towards Reliable Communications in Intelligent Reflecting Surface-Aided Cell-Free MIMO Systems

Rui Huang and Vincent W.S. Wong
Department of Electrical and Computer Engineering
The University of British Columbia, Vancouver, Canada
email: {ruihuang, vincentw}@ece.ubc.ca

Abstract—**Intelligent reflecting surface (IRS) and cell-free multiple-input multiple-output (CF-MIMO) systems are two promising multi-antenna technologies for the fifth generation and beyond (B5G) wireless communication systems. In this paper, we formulate a joint phase shift control and beamforming optimization problem to maximize the aggregate throughput subject to the reliability constraint of the users in an IRS-aided CF-MIMO system. We propose an alternating optimization (AO)-based algorithm, in which the joint problem is decomposed into a phase shift control subproblem and a beamforming subproblem. For the phase shift control subproblem, we propose a complex gradient descent (CGD)-based algorithm, which tackles the unit-modulus constraint and guarantees the aggregate throughput to be monotonic increasing in each iteration. We then propose a difference of convex programming (DCP)-based algorithm for beamforming optimization. Simulation results show that the proposed AO-based algorithm achieves an aggregate throughput that is 53.8% and 25.1% higher than the cellular MIMO system with zero-forcing beamformer and the IRS-aided CF-MIMO system with random phase shift control, respectively. Moreover, the reliability requirements of the users are satisfied with the proposed AO-based algorithm. Our results also demonstrate that the proposed algorithm improves the minimum throughput of the users and reduces the standard deviation of the throughput distribution.**

I. Introduction

The fifth generation and beyond (B5G) wireless communication system is a key enabler of those applications with stringent reliability requirement, including smart manufacturing, autonomous driving, and virtual reality [1]. These applications rely on the ultra-reliable information exchange between the base station and user equipment. Intelligent reflecting surface (IRS) and cell-free multiple-input multiple-output (CF-MIMO) systems have been recognized as novel multi-antenna techniques to improve the reliability of data transmission in B5G systems [2].

IRS is a planar surface equipped with a large number of passive reflecting elements. Each element can reflect the incident signal towards the receiver with a controllable phase shift. With a proper phase shift control of the reflecting elements, a higher signal-to-interference-plus-noise ratio (SINR) can be achieved at the receiver by enhancing the target signal and suppressing the interference [3]. In CF-MIMO systems, multiple base stations cooperate to serve the users by sharing the same physical resource block (PRB). This mitigates the inter-cell interference, alleviates the impact of handover, and improves the SINR of the cell-edge users [2].

The joint beamforming and phase shift control in an IRS-aided system has been studied in [4]–[6]. A parallel coordinate descent-based algorithm was proposed in [4] to optimize the phase shift of the IRS to mitigate the interference incurred by a secondary user. The authors in [5] formulated a sum-rate maximization problem in an IRS-aided cognitive radio system with an interference leakage constraint on the secondary users. The user scheduling problem in IRS-aided systems for mitigating the inter-user interference and maximizing the aggregate throughput has been investigated in [6].

The beamforming optimization and power control in CF-MIMO systems has been studied in [7]–[9]. The authors in [7] proposed power control algorithms to maximize the minimum SINR in downlink CF-MIMO systems by using conjugate beamforming and zero-forcing (ZF) beamforming. Maximizing the minimum SINR in uplink CF-MIMO systems was investigated in [8], and a geometric programming-based power control algorithm was proposed to obtain a suboptimal solution. The authors in [9] studied the power control for both uplink and downlink CF-MIMO systems for maximizing the aggregate throughput and the minimum data rate.

Given the existing research on CF-MIMO and IRS-aided systems, the following three challenges have not been fully addressed when considering reliable communication in IRS-aided CF-MIMO systems. First, the effects of channel dispersion and finite blocklength on the achievable reliability have not been considered in the aforementioned research. Due to channel dispersion and finite blocklength, the achievable data rate of a particular user can be lower than the rate determined based on Shannon capacity equation. Ignoring these effects in the problem formulation may lead to a potential violation of the reliability constraint in practice. Second, accounting for the channel dispersion and finite blocklength results in different SINR expressions and problem formulations. Some of the existing phase shift control algorithms, e.g., the fractional programming-based algorithm proposed in [6], rely on the *hidden convexity* of the phase shift control problem. However, such hidden convexity is not available when channel dispersion and finite blocklength are taken into account. Hence, the existing phase shift control algorithms need to be revisited to support reliable communications. Third, while the resource allocation in IRS-aided cellular systems has been studied in [4]–[6], the benefits of deploying an IRS in CF-MIMO systems have not been explored.

To address the aforementioned issues, in this paper, we study the joint beamforming optimization and phase shift control in a downlink IRS-aided CF-MIMO system. We aim to maximize the aggregate throughput subject to the reliability constraints of the users. The formulated problem is nonconvex due to the unit-modulus constraint that comes from the phase shift of the IRS, as well as the SINR expression incorporating the impact of channel dispersion and finite blocklength. To tackle these challenges, we propose an alternating optimization (AO)-based algorithm, in which complex gradient descent (CGD), Lagrangian method, difference of convex programming (DCP), and semidefinite programming (SDP) techniques are employed to transform and solve the formulated problem. Our contributions are as follows:

- We formulate a joint optimization problem for maximizing the aggregate throughput in an IRS-aided CF-MIMO system subject to the reliability constraint of the users. We propose an AO-based algorithm, in which the joint problem is decomposed into two subproblems for phase shift control and beamforming optimization, respectively.
- For the phase shift control subproblem, we propose a CGD-based algorithm, in which we exploit the gradient of the Lagrangian to tackle the unit-modulus constraint. We use a line search condition to ensure the monotonic increase of the objective function in each iteration.
- For the beamforming optimization subproblem, we relax the problem into a DCP problem and solve the problem using semidefinite relaxation (SDR).
- Simulation results show that, when the number of reflecting element is 140, the proposed AO-based algorithm achieves an aggregate throughput that is 53.8% and 25.1% higher than the cellular MIMO system with ZF beamformer, and the IRS-aided CF-MIMO system with random phase shift, respectively. Apart from satisfying the reliability requirements of the users, the proposed AO-based algorithm reduces the standard deviation of the throughput distribution among the users by up to 43.9% when compared with the cellular MIMO systems.

The remainder of this paper is organized as follows. The system model is given in Section II. The AO-based algorithm is proposed in Section III. Simulation results are presented in Section IV. Conclusions are drawn in Section V.

Notations: We use j to denote the imaginary unit. We use upper-case and lower-case boldface letters to denote matrices and column vectors, respectively. We use $\odot$ to denote the Hadamard product. $\mathbb{C}^{M\times N}$ denotes the set of $M \times N$ complex-valued matrices. $\boldsymbol{I}_M$ is an $M \times M$ identity matrix. $\boldsymbol{A}^T$, $\boldsymbol{A}^*$, $\boldsymbol{A}^H$, $\boldsymbol{A}^{-1}$ denote the transpose, conjugate, conjugate transpose, and inverse of matrix $\boldsymbol{A}$, respectively. $\text{diag}(\boldsymbol{x})$ returns a diagonal matrix where the diagonal elements are given by the elements of vector $\boldsymbol{x}$. $\text{rank}(\boldsymbol{A})$ and $\text{Tr}(\boldsymbol{A})$ return the rank and trace of matrix $\boldsymbol{A}$, respectively.

II. System Model

We consider the downlink transmission in an IRS-aided CF-MIMO system consisting of J base stations, one IRS, and N users. The base stations are connected to a central controller via backhaul channels. Each base station is equipped with K antennas, while each user has single antenna. For downlink transmission, the base stations share the same PRB to serve the users. An IRS with L_R reflecting elements is deployed to reflect the signals from the base stations to the intended users. An IRS-aided CF-MIMO system with two base stations and two users is shown in Fig. 1. We denote the set of users as $\mathcal{N}$, and the set of base stations as $\mathcal{J}$. We use $\psi_l \in [0, 2\pi)$, $l \in \{1, \dots, L_R\}$ to denote the phase shift of the l-th reflecting element on the IRS. We have the following unit-modulus constraint on the phase shift of the reflecting elements:

$$|e^{j\psi_l}| = 1,\ l \in \{1, \dots, L_R\}. \tag{1}$$

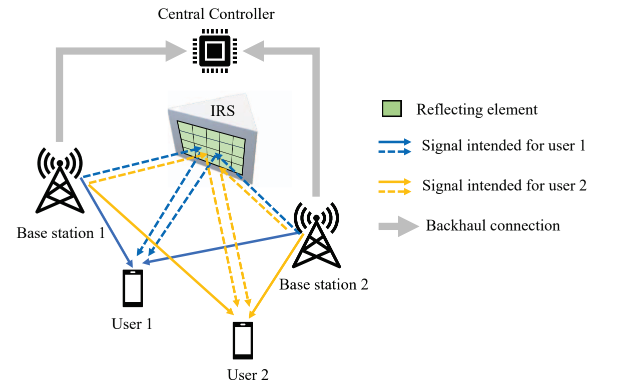

Fig. 1. An IRS-aided CF-MIMO system with two base stations sharing the same PRB to support downlink transmissions of two users.

The phase shift matrix of the IRS $\boldsymbol{\Psi}$ is defined as:

$$\boldsymbol{\Psi} = \text{diag}(e^{j\psi_1}, \dots, e^{j\psi_{L_R}}) \in \mathbb{C}^{L_R\times L_R}. \tag{2}$$

We use $\boldsymbol{h}_{\text{D},n,i} \in \mathbb{C}^K$ to denote the channel response between base station $i \in \mathcal{J}$ and user $n \in \mathcal{N}$ (i.e., the direct channel). We use $\boldsymbol{h}_{\text{R},n} \in \mathbb{C}^{L_R}$ to denote the channel response between the IRS and user n (i.e., the reflecting channel). The channel response between base station i and the IRS is denoted by $\boldsymbol{G}_i \in \mathbb{C}^{L_R\times K}$. We assume global channel state information is available at the base stations[1]. In addition, we assume block fading channels, where the channel responses are constant during the time period of the PRB.

The signal received by user $n \in \mathcal{N}$ is given by

$$y_n = \sum_{i\in\mathcal{J}} \big(\boldsymbol{h}^H_{\text{D},n,i}\, \boldsymbol{b}_{n,i}\, s_n + \boldsymbol{h}^H_{\text{R},n}\, \boldsymbol{\Psi}\, \boldsymbol{G}_i\, \boldsymbol{b}_{n,i} s_n\big) + I_n + z_n, \tag{3}$$

where $s_n \in \mathbb{C}$ is the symbol of user n with unit power, $\boldsymbol{b}_{n,i} \in \mathbb{C}^K$ is the beamforming vector of user n at base station i, z_n is the complex Gaussian noise with zero mean and variance σ^2. For user $n \in \mathcal{N}$, the term I_n denotes the interference from other users, which is given by

$$I_n = \sum_{m\in\mathcal{N}\setminus\{n\}} \sum_{i\in\mathcal{J}} \big(\boldsymbol{h}^H_{\text{D},n,i}\, \boldsymbol{b}_{m,i}\, s_m + \boldsymbol{h}^H_{\text{R},n}\, \boldsymbol{\Psi}\, \boldsymbol{G}_i\, \boldsymbol{b}_{m,i}\, s_m\big).$$

[1]We focus on the optimal performance that can be obtained with perfect channel estimation. The results present in this paper may serve as an upper bound of the real world performance of IRS-aided CF-MIMO systems.

We use $\boldsymbol{b} = \{\boldsymbol{b}_{n,i} \,|\, n \in \mathcal{N},\, i \in \mathcal{J}\}$ to collect the beamforming vectors of all users. The SINR of user $n \in \mathcal{N}$ is given by

$$\Gamma_n(\boldsymbol{\Psi}, \boldsymbol{b}) = \frac{\left|\sum_{i\in\mathcal{J}} \left(\boldsymbol{h}_{\mathrm{D},n,i}^H \boldsymbol{b}_{n,i} + \boldsymbol{h}_{\mathrm{R},n}^H \boldsymbol{\Psi} \boldsymbol{G}_i \boldsymbol{b}_{n,i}\right)\right|^2}{\sum_{m\in\mathcal{N}\setminus\{n\}} \left|\sum_{i\in\mathcal{J}} \left(\boldsymbol{h}_{\mathrm{D},n,i}^H \boldsymbol{b}_{m,i} + \boldsymbol{h}_{\mathrm{R},n}^H \boldsymbol{\Psi} \boldsymbol{G}_i \boldsymbol{b}_{m,i}\right)\right|^2 + \sigma^2}. \quad (4)$$

We assume all base stations have the same maximum downlink transmission power, which is denoted by $P^{\max}$. We have the following transmit power constraint:

$$\sum_{n\in\mathcal{N}} ||\boldsymbol{b}_{n,i}||_2^2 \le P^{\max},\ i \in \mathcal{J}. \quad (5)$$

We use $R_n(\boldsymbol{\Psi}, \boldsymbol{b})$ to denote the achievable throughput (bits/s/Hz) of user n. $R_n(\boldsymbol{\Psi}, \boldsymbol{b})$ is given by [10], [11]

$$R_n(\boldsymbol{\Psi}, \boldsymbol{b}) = \log_2(1 + \Gamma_n(\boldsymbol{\Psi}, \boldsymbol{b})) - D\sqrt{1 - \frac{1}{(1+\Gamma_n(\boldsymbol{\Psi}, \boldsymbol{b}))^2}}, \quad n \in \mathcal{N}, \quad (6)$$

where $D = \frac{\log_2(e)\, Q^{-1}(\epsilon)}{\sqrt{L}}$, ϵ is the target packet error rate, L is the packet length, and $Q^{-1}(\cdot)$ is the inverse Gaussian Q-function. The second term in (6) accounts for the effects of channel dispersion and finite blocklength [10]. We consider the following reliability requirement of user n [11]:

$$R_n(\boldsymbol{\Psi}, \boldsymbol{b}) \ge R_n^{\mathrm{req}},\ n \in \mathcal{N}, \quad (7)$$

where R_n^{req} denotes the minimum data rate in order to satisfy the reliability requirement of user n.

In this paper, we aim to maximize the aggregate throughput of the system subject to the reliability constraint of the users. This leads to the following optimization problem:

$$\begin{aligned} \underset{\boldsymbol{\Psi}, \boldsymbol{b}}{\text{maximize}} \quad & \sum_{n\in\mathcal{N}} R_n(\boldsymbol{\Psi}, \boldsymbol{b}) \\ \text{subject to} \quad & \text{constraints } (1),\ (5) \text{ and } (7). \end{aligned} \quad (8)$$

Problem (8) is nonconvex due to the objective function, the unit-modulus constraint in (1), and the reliability constraint in (7). In the next section, we propose an AO-based algorithm to obtain a suboptimal solution of problem (8).

III. AO-based Joint Beamforming and Phase Shift Optimization Algorithm

In this section, we propose an AO-based algorithm, in which the phase shift optimization and beamforming optimization are invoked iteratively to solve the joint problem.

A. CGD-based Phase Shift Control Algorithm

For the phase shift subproblem, we identify that the objective function is a real-valued function where the variable is the complex-valued matrix $\boldsymbol{\Psi}$. The nonconvexity of such objective function and the unit-modulus constraint can be tackled by the CGD method [12], [13].

We define vectors $\boldsymbol{\psi} = (\psi_1, \ldots, \psi_{L_R}, 0) \in \mathbb{R}^{L_R+1}$, and $\widehat{\boldsymbol{\psi}} = (e^{-j\psi_1}, \ldots, e^{-j\psi_{L_R}}, e^{j0}) \in \mathbb{C}^{L_R+1}$. Note that the first L_R elements in $\boldsymbol{\psi}$ and $\widehat{\boldsymbol{\psi}}$ correspond to the phase shift of the reflecting elements on the IRS, while the last element is introduced to incorporate the direct channels between the base stations and the users. Given the beamforming vector $\boldsymbol{b}$, we can rewrite the SINR of user $n \in \mathcal{N}$ as follows:

$$\Gamma_n(\boldsymbol{\psi}) = \Gamma_n(\widehat{\boldsymbol{\psi}}) = \frac{\widehat{\boldsymbol{\psi}}^H \boldsymbol{H}_n \widehat{\boldsymbol{\psi}}}{\widehat{\boldsymbol{\psi}}^H \boldsymbol{K}_n \widehat{\boldsymbol{\psi}}}, \quad (9)$$

where

$$\boldsymbol{H}_n = \widehat{\boldsymbol{H}}_n \widehat{\boldsymbol{H}}_n^H, \quad (10)$$

and

$$\widehat{\boldsymbol{H}}_n = \sum_{i\in\mathcal{J}} \begin{bmatrix} \mathrm{diag}(\boldsymbol{h}_{\mathrm{R},n}^H)\, \boldsymbol{G}_i \\ \boldsymbol{h}_{\mathrm{D},n,i}^H \end{bmatrix} \boldsymbol{b}_{n,i}.$$

The matrix $\boldsymbol{K}_n$ in (9) is given by

$$\boldsymbol{K}_n = \sum_{m\in\mathcal{N}\setminus\{n\}} \widehat{\boldsymbol{K}}_{n,m} \widehat{\boldsymbol{K}}_{n,m}^H + \frac{\sigma^2}{L_R+1} \boldsymbol{I}_{L_R+1}, \quad (11)$$

where

$$\widehat{\boldsymbol{K}}_{n,m} = \sum_{i\in\mathcal{J}} \begin{bmatrix} \mathrm{diag}(\boldsymbol{h}_{\mathrm{R},n}^H)\, \boldsymbol{G}_i \\ \boldsymbol{h}_{\mathrm{D},n,i}^H \end{bmatrix} \boldsymbol{b}_{m,i}, \quad m \in \mathcal{N}\setminus\{n\}.$$

To apply the CGD method to optimize the phase shift matrix, problem (8) needs to be reformulated as an unconstrained optimization problem. To this end, we rewrite constraint (1) as follows:

$$\psi_l \in \mathbb{R},\ l \in \{1, \ldots, L_R\}. \quad (12)$$

Constraints (1) and (12) are equivalent because

$$|e^{j\psi_l}| \overset{(a)}{=} |\cos(\psi_l) + j\sin(\psi_l)| = \sqrt{\cos^2(\psi_l) + \sin^2(\psi_l)} \overset{(b)}{=} 1.$$

Equality (*a*) follows from the Euler's formula, and equality (*b*) holds for all $\psi_l \in \mathbb{R}$. Given the beamforming vector $\boldsymbol{b}$, we use the following Lagrangian to account for the reliability requirement of the users in (7):

$$\mathcal{L}(\boldsymbol{\psi}, \boldsymbol{\lambda}) = \sum_{n\in\mathcal{N}} \left(\log_2(1+\Gamma_n(\boldsymbol{\psi})) - D\sqrt{1 - \frac{1}{(1+\Gamma_n(\boldsymbol{\psi}))^2}} \right) - \sum_{n\in\mathcal{N}} \lambda_n (R_n^{\mathrm{req}} - R_n(\boldsymbol{\psi})), \quad (13)$$

where $\lambda_n \ge 0$ is the Lagrange multiplier for the reliability constraint of user n, and vector $\boldsymbol{\lambda} = (\lambda_1, \ldots, \lambda_N)$.

The subproblem for phase shift control can be formulated as:

$$\underset{\psi_l\in\mathbb{R},\ l\in\{1,\ldots,L_R\},\ \boldsymbol{\lambda}\succeq\boldsymbol{0}}{\text{maximize}} \quad \mathcal{L}(\boldsymbol{\psi}, \boldsymbol{\lambda}). \quad (14)$$

The proposed CGD-based algorithm for solving problem (14) is shown in Algorithm 1. In Line 1, the phase shift of each reflecting element is initialized by drawing a random value from a uniform distribution over the interval $[x,\, x+2\pi)$, where x can be any arbitrary real number. This is because e^{jx}, $x \in \mathbb{R}$

Algorithm 1 The proposed CGD-based Algorithm for Phase Shift Optimization

1: Initialize phase shift $\boldsymbol{\psi}^{(0)}$ and Lagrange multipliers $\boldsymbol{\lambda}^{(0)}$.
2: Set iteration counter $t \leftarrow 0$.
3: Initialize the termination threshold ε_{CGD}.
4: **repeat**
5: Determine the gradient $\nabla_{\boldsymbol{\psi}} \mathcal{L}(\boldsymbol{\psi}^{(t)}, \boldsymbol{\lambda}^{(t)})$ based on (15).
6: Initialize the step size in backtracking line search as $\alpha_{\text{ls}}^{(0)}$.
7: Initialize the iteration counter for backtracking line search as $q \leftarrow 0$.
8: **while** $\mathcal{L}\left(\boldsymbol{\psi}^{(t)} + \alpha_{\text{ls}}^{(q)} \nabla_{\boldsymbol{\psi}} \mathcal{L}(\boldsymbol{\psi}^{(t)}, \boldsymbol{\lambda}^{(t)}), \boldsymbol{\lambda}^{(t)}\right) \geq \mathcal{L}(\boldsymbol{\psi}^{(t)}, \boldsymbol{\lambda}^{(t)}) + c\, \alpha_{\text{ls}}^{(q)} \nabla_{\boldsymbol{\psi}} \mathcal{L}(\boldsymbol{\psi}^{(t)}, \boldsymbol{\lambda}^{(t)})^T \nabla_{\boldsymbol{\psi}} \mathcal{L}(\boldsymbol{\psi}^{(t)}, \boldsymbol{\lambda}^{(t)})$ and $q \leq T^{\max}$ **do**
9: $\alpha_{\text{ls}}^{(q+1)} \leftarrow \beta\, \alpha_{\text{ls}}^{(q)}$.
10: $q \leftarrow q + 1$.
11: **end while**
12: $\alpha^{(t)} \leftarrow \alpha_{\text{ls}}^{(q)}$.
13: $\boldsymbol{\psi}^{(t+1)} \leftarrow \boldsymbol{\psi}^{(t)} + \alpha^{(t)} \nabla_{\boldsymbol{\psi}} \mathcal{L}(\boldsymbol{\psi}^{(t)}, \boldsymbol{\lambda}^{(t)})$.
14: $\boldsymbol{\lambda}^{(t+1)} \leftarrow \max\left\{\mathbf{0},\ \boldsymbol{\lambda}^{(t)} - \alpha^{(t)} \nabla_{\boldsymbol{\lambda}} \mathcal{L}(\boldsymbol{\psi}^{(t)}, \boldsymbol{\lambda}^{(t)})\right\}$.
15: $t \leftarrow t + 1$.
16: **until** $\left|\mathcal{L}(\boldsymbol{\psi}^{(t)}, \boldsymbol{\lambda}^{(t)}) - \mathcal{L}(\boldsymbol{\psi}^{(t-1)}, \boldsymbol{\lambda}^{(t-1)})\right| \leq \varepsilon_{\text{CGD}}$.

is a periodic function with a period of 2π. For example, both $[0,\, 2\pi)$ and $[-\pi,\, \pi)$ can be used for the initialization. In Line 5, we derive the gradient of $\mathcal{L}(\boldsymbol{\psi}, \boldsymbol{\lambda})$ as follows:

$$\begin{aligned} &\nabla_{\boldsymbol{\psi}} \mathcal{L}(\boldsymbol{\psi}, \boldsymbol{\lambda}) \\ &\quad = \sum_{n \in \mathcal{N}} 2\, C_n(\boldsymbol{\psi}) \boldsymbol{\nu}_n(\boldsymbol{\psi}) + \sum_{n \in \mathcal{N}} 2\, \lambda_n\, C_n(\boldsymbol{\psi})\, \boldsymbol{\nu}_n(\boldsymbol{\psi}) \\ &\quad = \sum_{n \in \mathcal{N}} 2\, (\lambda_n + 1)\, C_n(\boldsymbol{\psi})\, \boldsymbol{\nu}_n(\boldsymbol{\psi}), \end{aligned} \tag{15}$$

where vector $\boldsymbol{\nu}_n(\boldsymbol{\psi}) \in \mathbb{R}^{L_R+1}$ is given by

$$\begin{aligned} \boldsymbol{\nu}_n(\boldsymbol{\psi}) = \operatorname{Re}\Bigg\{ \Big(& \frac{\boldsymbol{H}_n^* \widehat{\boldsymbol{\psi}}^*}{\widehat{\boldsymbol{\psi}}^H \boldsymbol{K}_n \widehat{\boldsymbol{\psi}}} - \frac{(\widehat{\boldsymbol{\psi}}^H \boldsymbol{H}_n \widehat{\boldsymbol{\psi}})\, (\boldsymbol{K}_n^* \widehat{\boldsymbol{\psi}}^*)}{(\widehat{\boldsymbol{\psi}}^H \boldsymbol{K}_n \widehat{\boldsymbol{\psi}})^2} \Big) \\ & \odot \Big(\frac{\mathrm{d} e^{-j\psi_1}}{\mathrm{d}\psi_1}, \ldots, \frac{\mathrm{d} e^{-j\psi_{L_R}}}{\mathrm{d}\psi_{L_R}}, 0 \Big) \Bigg\}, \end{aligned}$$

and the term $C_n(\boldsymbol{\psi}) \in \mathbb{R}$ is given by

$$C_n(\boldsymbol{\psi}) = \Big(\frac{1}{\ln(2)(1 + \Gamma_n(\boldsymbol{\psi}))} - \frac{\mathrm{D}\, (1 + \Gamma_n(\boldsymbol{\psi}))^{-3}}{\sqrt{1 - (1 + \Gamma_n(\boldsymbol{\psi}))^{-2}}} \Big).$$

Based on the gradient $\nabla_{\boldsymbol{\psi}} \mathcal{L}(\boldsymbol{\psi}, \boldsymbol{\lambda})$, we update $\boldsymbol{\psi}$ in the t-th iteration of gradient descent as follows:

$$\boldsymbol{\psi}^{(t+1)} \leftarrow \boldsymbol{\psi}^{(t)} + \alpha^{(t)} \nabla_{\boldsymbol{\psi}} \mathcal{L}(\boldsymbol{\psi}^{(t)},\, \boldsymbol{\lambda}^{(t)}), \tag{16}$$

where $\alpha^{(t)}$ is the step size for gradient descent, and superscript (t) denotes the t-th iteration.

In Lines 6-12, we use the *Armijo condition* [14] and conduct line search to determine the step size $\alpha^{(t)}$ in the t-th iteration of gradient descent. In particular, we aim to find the step size $\alpha^{(t)}$ that satisfies the following Armijo condition [14]:

$$\begin{aligned} &\mathcal{L}\left(\boldsymbol{\psi}^{(t)} + \alpha^{(t)} \nabla_{\boldsymbol{\psi}} \mathcal{L}(\boldsymbol{\psi}^{(t)}, \boldsymbol{\lambda}^{(t)}), \boldsymbol{\lambda}^{(t)}\right) \\ &\geq \mathcal{L}(\boldsymbol{\psi}^{(t)}, \boldsymbol{\lambda}^{(t)}) + c\, \alpha^{(t)} \nabla_{\boldsymbol{\psi}} \mathcal{L}(\boldsymbol{\psi}^{(t)}, \boldsymbol{\lambda}^{(t)})^T \nabla_{\boldsymbol{\psi}} \mathcal{L}(\boldsymbol{\psi}^{(t)}, \boldsymbol{\lambda}^{(t)}), \end{aligned} \tag{17}$$

where $c > 0$ is a constant. In the backtracking line search, we initialize the step size α_{ls} as a predefined value $\alpha_{\text{ls}}^{(0)}$. In the q-th iteration of backtracking line search, we substitute $\alpha^{(t)}$ in (17) with $\alpha_{\text{ls}}^{(q)}$, and check if $\alpha_{\text{ls}}^{(q)}$ satisfies the condition. If $\alpha_{\text{ls}}^{(q)}$ satisfies the condition, then we update the step size in gradient descent as $\alpha^{(t)} \leftarrow \alpha_{\text{ls}}^{(q)}$. Note that, here t is the iteration counter for gradient descent, while q is the iteration counter for the backtracking line search. We use $\alpha^{(t)}$ to update the phase shift variables $\boldsymbol{\psi}$ based on (16). Otherwise, we continue the line search and update the step size in backtracking line search by

$$\alpha_{\text{ls}}^{(q+1)} \leftarrow \beta\, \alpha_{\text{ls}}^{(q)}, \tag{18}$$

where $\beta \in (0,\, 1)$ is a constant. We repeat the backtracking line search until constraint (17) is satisfied or a maximum number of iteration $T^{\max}$ is reached. In Line 14, we update the Lagrange multipliers using the following rule [15, Chap. 3]:

$$\boldsymbol{\lambda}^{(t+1)} \leftarrow \max\left\{\mathbf{0},\ \boldsymbol{\lambda}^{(t)} - \alpha^{(t)} \nabla_{\boldsymbol{\lambda}} \mathcal{L}(\boldsymbol{\psi}^{(t)}, \boldsymbol{\lambda}^{(t)})\right\}. \tag{19}$$

The termination condition of the CGD-based algorithm is shown in Line 16 of Algorithm 1. We repeat the gradient descent iteration until the improvement in the objective function is less than or equal to a predefined threshold ε_{CGD}.

B. Beamforming Optimization based on DCP

We first define vector $\boldsymbol{b}_n = (\boldsymbol{b}_{n,1}, \ldots, \boldsymbol{b}_{n,J}) \in \mathbb{C}^{JK},\ n \in \mathcal{N}$. We define matrix $\boldsymbol{B}_n = \boldsymbol{b}_n\, \boldsymbol{b}_n^H \in \mathbb{C}^{JK \times JK}$. Given the phase shift matrix $\boldsymbol{\Psi}$, the beamforming subproblem can be formulated as follows:

$$\begin{aligned} \underset{\gamma_n,\, \boldsymbol{B}_n,\, n \in \mathcal{N}}{\text{maximize}} \quad & \sum_{n \in \mathcal{N}} R_n(\gamma_n) \\ \text{subject to} \quad & \text{C1: } R_n(\gamma_n) \geq R_n^{\text{req}},\ n \in \mathcal{N}, \\ & \text{C2: } \gamma_n \leq \frac{\operatorname{Tr}(\widehat{\boldsymbol{H}}_n \boldsymbol{B}_n)}{\sum\limits_{m \in \mathcal{N} \setminus \{n\}} \operatorname{Tr}(\widehat{\boldsymbol{H}}_n \boldsymbol{B}_m) + \sigma^2},\ n \in \mathcal{N}, \\ & \text{C3: } \sum_{n \in \mathcal{N}} \operatorname{Tr}\left(\boldsymbol{B}_n \odot \boldsymbol{Q}_i\right) \leq P^{\max},\ i \in \mathcal{J}, \\ & \text{C4: } \boldsymbol{B}_n \succeq 0,\ n \in \mathcal{N}, \\ & \text{C5: } \operatorname{rank}(\boldsymbol{B}_n) \leq 1,\ n \in \mathcal{N}, \end{aligned} \tag{20}$$

where $R_n(\gamma_n) = \log_2(1 + \gamma_n) - D\sqrt{1 - \frac{1}{(1+\gamma_n)^2}}$, and $\gamma_n,\, n \in \mathcal{N}$ are the auxiliary variables. Matrix $\boldsymbol{Q}_i$ is a diagonal matrix in which the $((i-1)L+1)$-th to the iK-th diagonal elements are equal to 1, while all the remaining elements are equal to 0. Constraints C1 and C2 correspond to the reliability requirement of the users. Constraint C3 is the transmit power constraint of the base stations. Constraints C4 and C5 guarantee the decomposition $\boldsymbol{B}_n = \boldsymbol{b}_n\, \boldsymbol{b}_n^H$.

We note that, the beamforming subproblem (20) has a similar form as the beamforming problem in [11]. A suboptimal solution can be obtained based on DCP and SDR. Due to space limitation, we omit the presentation here and refer the readers to [11, Algorithm 3] for details.

Algorithm 2 AO-based Joint Beamforming and Phase Shift Optimization Algorithm

1: Initialize phase shift matrix $\mathbf{\Psi}$, and beamforming vector $\boldsymbol{b}$ as $\mathbf{\Psi}^{(0)}$ and $\boldsymbol{b}^{(0)}$, respectively.
2: Initialize the AO termination threshold ε_{AO}.
3: Initialize the iteration counter $t \leftarrow 0$.
4: **repeat**
5: Determine the beamforming vector $\boldsymbol{b}_n^{(t+1)}$ for each user $n \in \mathcal{N}$ using DCP for given phase shift matrix $\mathbf{\Psi}^{(t)}$.
6: Determine the phase shift matrix $\mathbf{\Psi}^{(t+1)}$ using the proposed CGD-based algorithm for given beamforming vector $\boldsymbol{b}^{(t+1)}$.
7: $t \leftarrow t+1$.
8: **until** $\left|\sum_{n\in\mathcal{N}}\left(R_n(\mathbf{\Psi}^{(t+1)},\boldsymbol{b}^{(t+1)}) - R_n(\mathbf{\Psi}^{(t)},\boldsymbol{b}^{(t)})\right)\right| \leq \varepsilon_{\text{AO}}$.

C. Overall AO-based Algorithm for Joint Optimization

The proposed AO-based algorithm is shown in Algorithm 2. In Line 5, in each AO iteration, we solve the beamforming subproblem using DCP with the given phase shift matrix. In Line 6, after updating the beamforming vectors, we use the proposed CGD-based algorithm to solve the phase shift control subproblem. In Line 8, the iterative process is repeated until the objective function in (8) converges.

We justify the convergence of the proposed AO-based algorithm as follows. In the proposed CGD-based algorithm for phase shift optimization, the objective function is monotonically increasing after each iteration in Algorithm 1. This is because the backtracking line search guarantees an improvement in the objective function in each iteration. Moreover, solving the beamforming subproblem using DCP results in a sequence of convex optimization problems that converge to a stationary point of the beamforming subproblem [16, Theorem 3]. Hence, the proposed AO-based algorithm in Algorithm 2 is guaranteed to converge to a stationary point of the joint problem [17].

IV. Performance Evaluation

We simulate an IRS-aided CF-MIMO system with $J = 2$ base stations and one IRS over a two-dimensional plane. The two base stations are located at $(0, 0)$ and $(100, 0)$, respectively. The coordinate of the IRS is $(50, 10)$. The users are randomly distributed within a 120° annulus sector where the IRS is located at the center of the sector. The inner radius of the annulus sector is 5 m and the outer radius is 15 m. Other simulation parameters are shown in Table I. The results are averaged over 100 different channel realizations. We compare the performance of the proposed AO-based algorithm with the following baseline algorithms:

- Cellular MIMO systems with coordinated beamforming and fixed phase shift control: In this algorithm, the base stations employ a multicell ZF beamformer [18] to mitigate the interference. We set the phase shifts of all reflecting elements on the IRS to be equal to zero.
- CF-MIMO systems with the proposed DCP-based beamforming optimization and random phase shift: In this algorithm, the phase shift of each reflecting element is determined independently by drawing a random value from a uniform distribution over the interval $[0, 2\pi)$. The proposed DCP-based algorithm is invoked to optimize the beamforming vectors.

TABLE I
Simulation Parameters

Parameter	Value
Carrier frequency	2.4 GHz
Minimum throughput to satisfy the reliability requirement R_n^{req}, $n \in \mathcal{N}$	5 bits/s/Hz
Path loss exponent of direct channels (Rayleigh fading)	3.5 [19]
Path loss exponent of reflecting channels (Rician fading)	2 [19]
Rician K-factor of reflecting channels	6 [19]
Maximum transmit power $P^{\max}$	30 dBm
Noise power of downlink channel σ^2	-90 dBm
Constant c in the Armijo condition	5×10^{-4}
Constant β in CGD	0.5
Initial step size α_{ini} in CGD	1
Maximum iteration in backtracking line search $T^{\max}$	20
Termination threshold for the CGD-based algorithm ε_{CGD}	1×10^{-3}
Termination threshold for the proposed AO-based algorithm ε_{AO}	5×10^{-3}

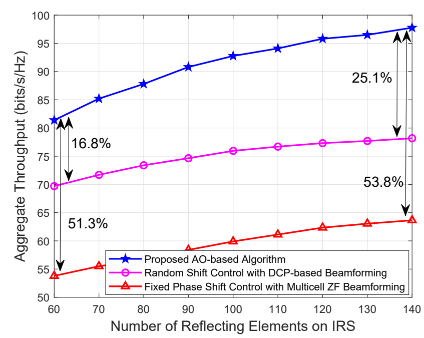

Fig. 2. Aggregate throughput versus the number of reflecting elements. We set $N = 8$ and $K = 8$.

In Fig. 2, we show the aggregate throughput versus the number of reflecting elements L_R on the IRS. The results show that the users achieve a higher aggregate throughput in CF-MIMO systems when compared with cellular MIMO systems. Moreover, we observe a greater increment in the aggregate throughput of the proposed AO-based algorithm as L_R increases, when compared with the baseline algorithms. This is because the phase shift matrix of the IRS is jointly optimized with the beamforming vectors in the proposed AO-based algorithm. In particular, when L_R is equal to 140, the aggregate throughput of the proposed AO-based algorithm is 25.1% and 53.8% higher than the random phase shift control with DCP-based beamforming and the fixed phase shift control with multicell ZF beamforming, respectively.

In Fig. 3, we show the aggregate throughput versus the number of antennas K. The proposed AO-based algorithm achieves the highest aggregate throughput when K varies from 8 to 16. In particular, when K is equal to 8, the proposed AO-based algorithm achieves an aggregate throughput that is 23.4% and 54.6% higher than the random phase shift control with DCP-based beamforming and the fixed phase

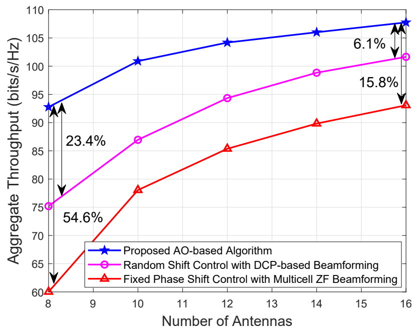

Fig. 3. Aggregate throughput versus the number of antennas. We set $N = 8$ and $L_R = 100$.

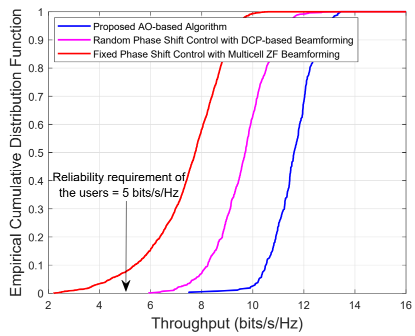

Fig. 4. Empirical cumulative distribution function of the throughput. We set $N = 8$, $K = 8$, and $L_R = 100$.

shift control with multicell ZF beamforming, respectively. We also observe that all considered algorithms benefit from having more antennas at the base stations. This is in line with the fact that more antennas provides a higher degrees of freedom in both CF-MIMO and cellular MIMO systems. These extra degrees of freedom can be exploited to mitigate the interference and improve the aggregate throughput.

We show the empirical cumulative distribution function of the throughput distribution among the users in Fig. 4. The minimum throughput with the proposed AO-based algorithm and the random phase shift control with DCP-based beamforming algorithm are 7.5 bits/s/Hz and 5.9 bits/s/Hz, respectively. All users satisfy the reliability requirement with the proposed AO-based algorithm and the random phase shift control with DCP-based beamforming algorithm. However, 7.3% of the users cannot satisfy the reliability requirement with the fixed phase shift control with multicell ZF beamforming algorithm. Moreover, the standard deviation of the throughput distribution with the proposed AO-based algorithm is 22.6% and 43.9% lower than the random phase shift control with DCP-based beamforming and the fixed phase shift control with multicell ZF beamforming, respectively.

V. Conclusion

In this paper, we proposed an AO-based algorithm for maximizing the aggregate throughput of the IRS-aided CF-MIMO systems with the reliability constraint of the users. We transformed the phase shift subproblem into an unconstrained optimization problem using the Lagrangian method, and proposed a CGD-based algorithm to solve the problem. We formulated the beamforming subproblem as a DCP problem and obtained a suboptimal solution. Our results showed that the proposed AO-based algorithm can achieve a higher aggregate throughput compared with two baseline algorithms. Moreover, the reliability requirements of the users can be satisfied with the proposed AO-based algorithm. The proposed AO-based algorithm also reduces the standard deviation of the throughput distribution among the users. For future work, extending the current model by considering the CF-MIMO systems with multiple IRSs is a promising topic.

References

[1] M. Bennis, M. Debbah, and H. V. Poor, "Ultrareliable and low-latency wireless communication: Tail, risk, and scale," *Proceedings of the IEEE*, vol. 106, no. 10, pp. 1834–1853, Oct. 2018.

[2] J. Zhang, E. Björnson, M. Matthaiou, D. W. K. Ng, H. Yang, and D. J. Love, "Prospective multiple antenna technologies for beyond 5G," *IEEE J. Sel. Areas Commun.*, vol. 38, no. 8, pp. 1637–1660, Aug. 2020.

[3] Q. Wu and R. Zhang, "Intelligent reflecting surface enhanced wireless network via joint active and passive beamforming," *IEEE Trans. Wireless Commun.*, vol. 18, no. 11, pp. 5394–5409, Nov. 2019.

[4] Y. Jia, C. Ye, and Y. Cui, "Analysis and optimization of an intelligent reflecting surface-assisted system with interference," *IEEE Trans. Wireless Commun.*, vol. 19, no. 12, pp. 8068–8082, Dec. 2020.

[5] D. Xu, X. Yu, and R. Schober, "Resource allocation for intelligent reflecting surface-assisted cognitive radio networks," in *Proc. of IEEE Int'l Workshop Signal Process. Advances Wireless Commun.*, May 2020.

[6] R. Huang and V. W. S. Wong, "Neural combinatorial optimization for throughput maximization in IRS-aided systems," in *Proc. of IEEE Global Commun. Conf. (GLOBECOM)*, Taipei, Taiwan, Dec. 2020.

[7] E. Nayebi, A. Ashikhmin, T. L. Marzetta, H. Yang, and B. D. Rao, "Precoding and power optimization in cell-free massive MIMO systems," *IEEE Trans. Wireless Commun.*, vol. 16, no. 7, pp. 4445–4459, Jul. 2017.

[8] M. Bashar, K. Cumanan, A. G. Burr, M. Debbah, and H. Q. Ngo, "On the uplink max–min SINR of cell-free massive MIMO systems," *IEEE Trans. Wireless Commun.*, vol. 18, no. 4, pp. 2021–2036, Apr. 2019.

[9] S. Buzzi, C. D′Andrea, A. Zappone, and C. D′Elia, "User-centric 5G cellular networks: Resource allocation and comparison with the cell-free massive MIMO approach," *IEEE Trans. Wireless Commun.*, vol. 19, no. 2, pp. 1250–1264, Feb. 2020.

[10] M. K. Abdel-Aziz, S. Samarakoon, C. Liu, M. Bennis, and W. Saad, "Optimized age of information tail for ultra-reliable low-latency communications in vehicular networks," *IEEE Trans. Commun.*, vol. 68, no. 3, pp. 1911–1924, Mar. 2020.

[11] W. R. Ghanem, V. Jamali, Y. Sun, and R. Schober, "Resource allocation for multi-user downlink MISO OFDMA-URLLC systems," *IEEE Trans. Commun.*, vol. 68, no. 11, pp. 7184–7200, Nov. 2020.

[12] A. Hjorungnes, *Complex-Valued Matrix Derivatives: With Applications in Signal Processing and Communications*. Cambridge University Press, 2011.

[13] K. Kreutz-Delgado, "The complex gradient operator and the CR-Calculus," *arXiv preprint arXiv:2004.12957*, Jun. 2009.

[14] J. Nocedal and S. Wright, *Numerical Optimization*. Springer Science & Business Media, 2006.

[15] D. P. Bertsekas, *Constrained Optimization and Lagrange Multiplier Methods*. Academic Press, 2014.

[16] P. D. Tao and L. T. H. An, "Convex analysis approach to DC programming: Theory, algorithms and applications," *Acta Mathematica Vietnamica*, vol. 22, no. 1, pp. 289–355, Dec. 1997.

[17] J. C. Bezdek and R. J. Hathaway, "Convergence of alternating optimization," *Neural, Parallel Sci. Comput.*, vol. 11, pp. 351–368, Dec. 2003.

[18] O. Somekh, O. Simeone, Y. Bar-Ness, A. M. Haimovich, and S. Shamai, "Cooperative multicell zero-forcing beamforming in cellular downlink channels," *IEEE Trans. Inf. Theory*, vol. 55, no. 7, pp. 3206–3219, Jul. 2009.

[19] 3GPP TR 38.901 V16.1.0, "Technical specification group radio access network; Study on channel model for frequencies from 0.5 to 100 GHz (Release 16)," Dec. 2019.